ELSEVIER

Bioelectrochemistry and Bioenergetics 35 (1994) 39–47

BIOELECTROCHEMISTRY AND BIOENERGETICS

Modelling of the effect of a weak electric field on a nonlinear transmembrane ion transfer system

G.Yu. Riznichenko *, T.Yu. Plusnina, S.I. Aksyonov

Biological Faculty of Moscow State University, 119899 Moscow, Russian Federation

Abstract

A mathematical modelling of the K^+/H^+ antiport system was carried out to investigate the influence of a weak low-frequency applied periodic electric field on ion flux via a carrier across the lipid membrane. Nonlinear in character, the system can have a damped oscillatory, trigger or self-sustained oscillatory behaviour depending on the pattern of the ionic flux. Numerical calculation showed that the applied electric field could parametrically regulate nonlinear biological systems and the effects can be significant in bifurcation areas. The intensity of applied periodic electric field was estimated to be in the range 10–600 V cm^{-1} and the frequency in the range 10^{-2}–10 Hz.

Keywords: Weak electric field; Nonlinear transmembrane ion transfer

1. Introduction

The influence of weak low-frequency electromagnetic fields on living organisms has long been, and still is, a problem of interest to investigators. Ten years ago the question was whether such fields do exert an influence on living organisms. The major problem nowadays is the understanding of its mechanisms.

A wealth of approaches to the problem have been proposed in the literature and can be divided into two groups: "energetic" and "informational". The first-group mechanisms are those where the absorption of electromagnetic energy by molecules or structures of higher order is followed by electron excitation or by a conformation transition, or by the formation of dipoles, etc. [1–6]. These mechanisms, however, are inadequate to explain the effects of extremely low-amplitude, low-frequency electromagnetic exposures. In contrast, the adherents to the "informational" approach consider an electromagnetic signal as a piece of information conveyed to living system [7–10]. The energy of the signal can be very small and all the subsequent conversions in the system are implemented using the energy of the system itself, produced as a result of naturally occurring processes.

We shall draw attention here to some specific responses of biological systems observed in experiments. A response is evident, or exists, only in certain (sometimes very narrow) ranges of frequencies and/or amplitudes. The biological effects are not proportional to the intensity of the applied field and are of a threshold kind of pattern. The nonlinear character of such effects has been reported [11–13]. Our view is that nonlinearity is not a mere characteristic of the biological property of a living system, being out of equilibrium thermodynamically. It is a property due to which "small" exposures can bring about "large" responses. In terms of nonlinearity, the major cause of the observed responses to weak electromagnetic signals, the specific behaviour of biological systems mentioned above, can adequately be explained. The "informativity", the major tenet of the concept, arises from the fact that applied field affects the parameters of the system, rather than its structure elements. This is important to emphasize. Because of the structural stability of the biological systems, a small perturbation cannot usually bring it out of homeostasis. However, in the neighbourhood of the bifurcation boundaries of the parameters, a perturbation of these parameters can cause sharp changes in the kinetic structure and function of the system. In this paper we shall illustrate this using three nonlinear models of ion transport systems.

Many investigators of weak electromagnetic expo-

* Corresponding author.

Elsevier Science S.A.
SSDI 0302-4598(94)01729-K

sures believe that membranes and adjacent areas abundant in ion flows are targets for an attack of electromagnetic fields [1–3,5,6,14]. Indeed, the solid-to-liquid interface is a premise for the occurrence of nonlinear processes in the membrane and adjacent to it, and the parameters of the ion flux may be a target for an electromagnetic attack. Experimental data are available from studies in which ion flows were subjected directly to weak electromagnetic fields [15–17]. To illustrate our approach, we constructed models of transmembrane ion transport, each with its own type of nonlinearity.

2. Mathematic modelling and computer simulation

2.1. Effect of variable electric field on K^+/H^+ antiport system, a kind of resonant system

The first of our models considers a resonance response of the system to the applied electric field. The principal features which distinguish our approach from approaches of other resonance models (e.g. the model of Tsong and co-workers [5,6,11]) are discussed below.

Let consider an open transmembrane ion transport system in which proton H^+ and potassium ion K^+ flux flow in and out of the near-membrane layer (V_H and V_K are influx rates; $k_H[H^+]$ and $k_K[K^+]$ are outflux rates) and their antiport via carrier T^- (Eq. (1)). To be certain, we take nigericin as a carrier, known for its two sites of binding: one for a proton, H^+, and the other for a K^+ ion.

In constructing the kinetic model of ion transfer across the membrane, we use the following assumptions:

the T^-carrier can mediate proton and ion transport in the form of both neutral TH and TK complexes and a charged THK^+ complex:

the affinity constant is much larger for a TH–K^+ complex than for a T–K complex [18]; a K^+ ion cannot force H^+ out of a TH complex, and for that reason it is transferred in a protonated form of complex, TH–K^+.

With the above assumptions, the kinetic diagram for the antiport can be presented as

$$\begin{array}{r|c|l}
V_H \longrightarrow H^+ + \;{}^{1} & T^- \underset{k_{-1}}{\overset{k_{+1}}{\rightleftharpoons}} TH \xrightarrow{k_{+2}} T^- & {}^{2}\; +H_2^+ \xrightarrow{k_H} \\
\xleftarrow{k_K} K_1^+ + & TH \xleftarrow{k_{+4}} THK^+ \underset{k_{-3}}{\overset{k_{+3}}{\rightleftharpoons}} TH & +K_2^+ \longleftarrow V_K
\end{array} \tag{1}$$

where subscripts 1 and 2 on ion concentrations represent the solution on each side of the membrane, $k_{\pm i}$ $(i = 1, 3)$ are rate constants of association and dissociation of the ion-transporter complex and k_i $(i = 2, 4)$ are effective constants of the complex translocation and dissociation.

The system of equations describing the above reactions takes the form

$$\begin{aligned}
&d[H_1^+]/dt = V_H - k_{+1}[H_1^+][T^-] + k_{-1}[TH] \\
&d[K_2^+]/dt = V_K - k_{+3}[K_2^+][TH] + k_{-3}[THK^+] \\
&d[T^-]/dt = -k_{+1}[H_1^+][T^-] + k_{-1}[TH] + k_{+2}[TH] \\
&d[THK^+]/dt = k_{+3}[TH][K_2^+] - k_{-3}[THK^+] \\
&\qquad\qquad - k_{+4}[THK^+] \\
&[T^-] + [TH] + [THK^+] = T_0
\end{aligned} \tag{2}$$

where T_0 in the last mass conservation equation is the overall transporter concentration. We pass then to dimensionless variables: $x = [H_1^+]/K_m$, $y = [K_2^+]/\bar{K}_m$, $\tau = tT_0k_{+4}/\bar{K}_m$, where $\bar{K}_m = (k_{-3} + k_{+4})/k_{+3}$, $K_m = (k_{-1} + k_{+2})/k_{+1}$ and parameters $\epsilon = T_0/\bar{K}_m$, $V_H = V_H\bar{K}_m/(k_{+4}T_0K_m)$, $V_K = V_K/(k_{+4}T_0)$, $a = \bar{K}_mk_{+2}/(K_mk_{+4})$.

Assuming $T_0 \ll K_m$ allows one to introduce the hierarchy of times and thereby to facilitate the system of differential equations. In the limit transition, as $\epsilon \to 0$, the system of differential equations within dimensionless variables using the above denotations is recast in the form

$$\begin{aligned}
&dx/d\tau = V_H - ax/(1 + x + xy) \\
&dy/d\tau = V_K - yx/(1 + x + xy)
\end{aligned} \tag{3}$$

The steady-state values of x and y are

$$\bar{X} = V_H/[a(1 - V_K) - V_H], \qquad \bar{y} = V_Ka/V_H$$

Solving the characteristic equation of the linearized system yields the condition for a focus-type steady state:

$$\begin{aligned}
&V_H(1 - V_K) + [a(1 - V_K) - V_H]^2 \\
&\quad < 2V_H^{1/2}[a(1 - V_K) - V_H]
\end{aligned}$$

With parameters agreeing with this condition, damped oscillation of ion concentrations takes place (Fig. 1, curve 1)

In describing the flow of charged particles in the near-membrane layer and across the membrane, we used the Nernst–Plank equation for electrically driven diffusion:

$$J = uRT\ dc/ds - uczF\ d\phi/ds \tag{4}$$

and the linear approximation of the Poisson–Bolzmann equation:

$$d^2\phi/ds^2 = \kappa^2\phi, \qquad \kappa^2 = 8\pi c_e z_e^2 F^2/(RT\epsilon_d)$$

where z is the ion valence, T is absolute temperature, R is the gas constant, F is the Faraday constant, u is the mobility of ions whose concentration is c in plane

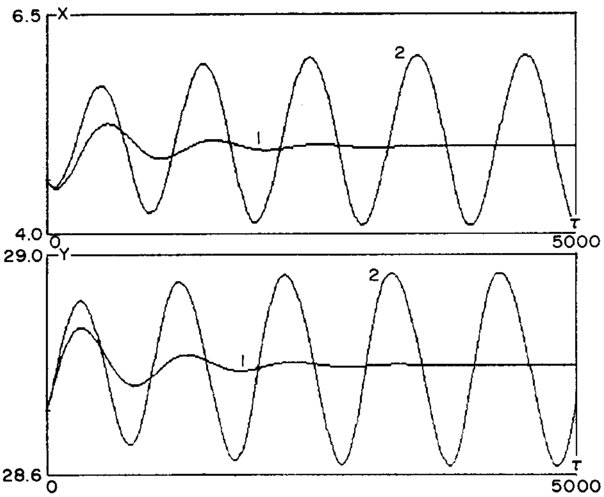

Fig. 1. Computer simulation of kinetics of a resonance system [7]. x, y, τ = Proton [H^+] and potassium [K^+] concentrations and time, respectively. Curves 1, internal damped concentration oscillations in K^+/H^+ antiport. Curves 2, imposed by electric field concentration oscillations in resonance in K^+/H^+ antiport. Amplitude of applied electric field $A = 0.0005$; resonance frequency $\omega = 0.0064$. Parameters used: $V_H = 1$, $V_K = 0.96$, $a = 30$.

s, c_e is the electrolyte concentration, z_e is the electrolyte charge and ϵ_d is the dielectric constant.

Let the potential gradient $d\phi$ in plane s be constant for the membrane: $d\phi/ds$ = constant (the assumption is valid for a thin membrane) and $d\phi/ds$ = constant be true for the near-membrane layer. Let the ion concentration gradient be constant in the near-membrane layer and across the membrane: dc/ds = constant. This allows one to represent the continuity Eq. (4) in the form of the ion concentration rate:

$$V = dc/dt = uczF\kappa^2\phi \qquad (5)$$

Thus the rate of ion inflow into the near-membrane area is linearly dependent on potential. Under a periodic sinusoidal pattern of applied electric field, the ion flow rate will vary as

$$V_H(1 + A \sin \omega\tau), \qquad V_K(1 + A \sin \omega\tau)$$

where A is the dimensionless amplitude and ω is the dimensionless cyclic frequency of applied electric signal. The amplitude reflects the relative proportion of the strengths of the applied and the internal field in the near-membrane region.

For the system in an applied field, Eq. (3) take the form

$$dx/d\tau = V_H(1 + A \sin \omega\tau) - ax/(1 + x + xy)$$
$$dy/d\tau = V_K(1 + A \sin \omega\tau) - yx/(1 + x + xy) \qquad (6)$$

With the applied field being of a small amplitude, $A = 0.0005$, and a frequency close to that of damped oscillation in the non-perturbed system (3), system (6) gives a resonant response (Fig. 1, curve 2). Its frequency response is presented in Fig. 2. It shows a drastic dependence of the amplitude ΔH^+ of proton oscillations on the frequency of the applied field, and a weaker one ΔK^+ for potassium ion oscillations. The difference between the H^+ and K^+ ion frequency response may be due to the difference in the H^+ and K^+ mobilities. Within the ranges of variation of the parameters considered in the model, namely, $V_H = 0.01$ to 100, $V_K = 0.96$ to 0.99 and $a = 0.75$ to 10 100, the resonance cyclic frequency changes within an order of magnitude: $\omega_r = 4.9 \times 10^{-4}$ to 7.5×10^{-3}.

To determine the resonance frequency of external exposure in dimensional form, we estimated the eigenfrequency f of the system in dimensional form:

$$f = \omega_0 T_0 k_{+4}/2\pi\bar{K}_m$$

with constants T_0, k_{+4} and $\bar{K}_m$ defined as above and ω_0 is the eigen cyclic frequency, $\omega_0 \approx \omega_r$.

When the ion transfer across the membrane is a limiting stage, k_{+4} and the rate constant of the transmembrane ion transfer are of the same order of magnitude. As $k_{-3} \gg k_{+4}$, the expression for $\bar{K}_m$ becomes

$$\bar{K}_m = (k_{-3} + k_{+4})/k_{+3} \approx k_{-3}/k_{+3}$$

The $\bar{K}_m$ value for nigericin can be of the order of 10^{-6} M, according to Ref. [19]. In Ref. [20], the value of k_{+4} for nigericin was estimated to be 1.7×10^4 s^{-1}. For a concentration of the carrier of $T_0 = 10^{-7}$ M, $f \approx 1.3 \times 10^{-2}$–2 Hz.

Hence the eigenfrequency of the system (and consequently the resonance frequency of the applied field) falls within the extremely low frequency range. In numerical experiments, the strength of the applied electric field was 0.0005 of that in the near-membrane

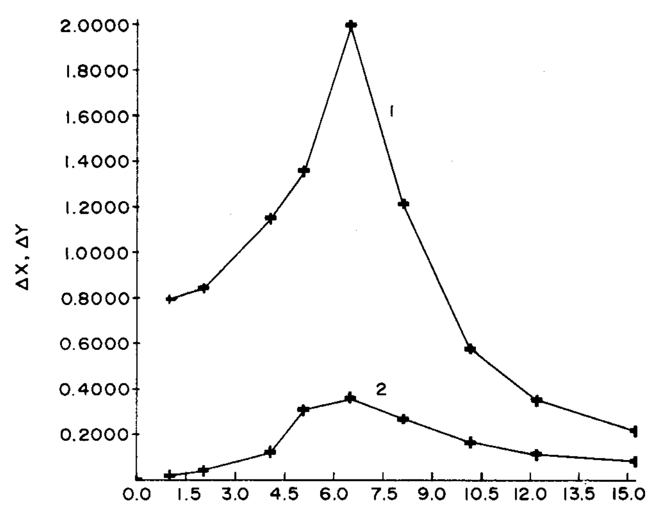

Fig. 2. Amplitude–frequency response for proton (curve 1) and potassium ion (curve 2) concentrations. Δx, Δy = Amplitudes of proton and potassium ion concentration oscillations, respectively, as functions of frequency ω of applied electric field.

area. If the membrane voltage is about 10 mV, which corresponds to 2×10^4 V cm^{-1} [5], the intensity of the applied field is 10 V cm^{-1}.

This estimate of electric field strength is nearly the same as that used in the experiments by Tsong and co-workers [15–17]. The frequency of the applied field was 1 kHz–1 MHz, which was reflected in the electroconformation coupling (ECC) model [5]. As mentioned above, in our model the key effect is resonance, as in the ECC model. However, there is an important, difference of principle which allows one to explain the lower frequency exposures used in other experiments [21,22]. In the ECC model, the energy necessary to produce this effect comes from outside, owing to the applied electric field. At resonance it is "pumped" into the system. As our system is open, and at all time ions flow into it (Eq. (1), terms V_H and V_K), energy comes in this way, i.e. most of the energy used in the effects in question is generated by the living system itself. The effect of the periodic electric field is presented as a small additional term $A\sin(\omega\tau)$ in Eq. (5) where $A = 0.0005 \ll 1$. In this situation the function of the applied electric field is to modulate the ion influx rate, that is, it is informational in character.

Another feature, which is different from the above-mentioned ECC model, is that the external field is applied to the near-membrane region, not the intra-membrane region. As seen from the kinetics, the rates of the intra-membrane processes, although dependent on potential because the carrier may be charged, are not limiting. This is a quasi-equilibrium situation. Briefly, this means that the intra-membrane ion transport processes are fast and a low-frequency field cannot "catch up" with them to produce its effect. It should be noted that the authors of Refs. [23,24] pointed out a greater probability of the influence of applied field on the processes in the near-membrane region, rather than on the conformation transition of the carriers.

2.2. *Effect of a periodic perturbation on a multi-stable transmembrane ion transport system*

We have considered above a K^+/H^+ antiport model in which there is a stable focal point. A system of this kind can amplify weak external periodic action at frequencies close to the natural frequency of the system. That is, it can act as a sort of resonance amplifier. Systems of another type, e.g. systems having more than one stable steady state, can also change their state significantly under a weak periodic exposure. A phenomenon of specific interest is parametric frequency regulation, when there is a critical frequency of the weak external signal capable of switching the system to a state other than the initial steady state. A flip-flop-like behaviour can be observed with differently modified transmembrane ion transport systems. In particular, the system in Eqs. (1) becomes bistable when the protonated carrier can bind another proton to the binding site of ion K^+ and the complex formed cannot be transferred across the membrane. A scheme of the reactions in this system is shown in Eqs. (7).

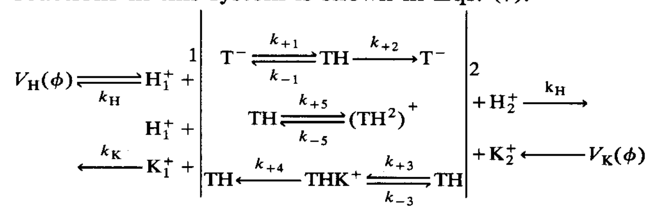

(7)

where subscripts 1 and 2 on ion concentrations represent the two sides of the membrane. $k_{\pm i}$ $(i = 1, 3, 5)$ are rate constants of association and dissociation of the ion-transporter complex; k_i $(i = 2, 4)$ are effective constants of the complex translocation and dissociation. Using a system of equations analogous to Eq. (2) with dimensionless variables and a proper hierarchy of times, one obtains

$$dx/d\tau = V_H - k_H x - ax/(1 + x + xy + bx)$$

$$dy/d\tau = V_K - yx/(1 + x + xy + bx) \qquad (8)$$

where $a = \bar{K}_m k_{+2}/(K_m k_{+4})$, $\bar{K}_m = (k_{-3} + k_{+4})/k_{+3}$, $K_m = (k_{-1} + k_{+2})/k_{+1}$, $b = K_m k_{+5}/k_{-5}$.

The steady-state solution is derived from the equations

$$\bar{y} = V_K a/(V_H - k_H \bar{x})$$

$$V_H - k_H\bar{x} - a\bar{x}/\left(1 + \bar{x} + b\bar{x} + V_K a\bar{x}/(V_H - k_H\bar{x})\right) = 0$$

For proton concentration, the steady-state solution $\bar{x}$ can be derived from the third-degree equation

$$-bk_H(\bar{x})^3 + (\bar{x})^2(bV_H - k_H)$$
$$-\bar{x}(k_H - V_K a + a - V_H) + V_H = 0 \qquad (9)$$

Depending on the sign of the discriminant, Eq. (9) can have one, two or three positive roots. The latter situation reflects three steady states of the system, two stable points and one unstable point (Fig. 3). The system can assume one of the two stable states, depending on the initial concentrations of the ions. The system can be controlled by varying the rates of ion inflows V_H and V_K to domains. There is a narrow parametric region in which the system operates in a flip-flop manner (Fig. 4(a,b)). For V_H there are two edge bifurcation values in the positive region, V_{H1} and V_{H2} (Fig. 4(a)) and for V_K one bifurcation value V_{K1} (Fig. 4(b)). In the presence of applied exposure, the system of Eq. (8) takes the form

$$dx/d\tau = V_H(1 + A\sin\omega\tau) - k_H x$$
$$- ax/(1 + x + xy + bx)$$
$$dy/d\tau = V_K(1 + A\sin\omega\tau) - yx/(1 + x + xy + bx)$$

(10)

The results of computer simulation show the following. With a fixed amplitude of $A = 0.03$ of the applied exposures the frequency was varied in the range $\omega = 0.01–0.1$. Within this range, with two critical values of the frequency, $\omega_1 = 0.047$ and $\omega_2 = 0.023$ were found.

With a fixed amplitude and a high frequency $\omega = 0.1$ of the exposure, the system oscillates with small amplitude around one of the steady states according to initial conditions (Fig. 5(a)). On reaching the value ω_1, the system assumes a configuration with a single stable state (3) irrespective of the initial conditions. When movement begins somewhere in the vicinity of state (1), a switching to the state (3) occurs (Fig. 5(b)). One can explain a switching to only one direction by the following. With ω_1 the period of the applied perturbation is larger than the time of the transition from state (1) to state (3) and smaller than the time of the backward transition.

On reaching the second critical frequency ω_2, the system enters into oscillations between two stable states (1) and (3). Now the period of the applied perturbation is larger than both the time of the direct transitions and the time of the backward transition. Hence the periodic transitions between two states take place (Fig. 5(c)).

The technique used to estimate the applied field frequency and intensity in dimensional form was that employed previously for a resonant oscillatory system: $f = \omega_0 T_0 k_{+4} / 2\pi \overline{K}_m$, where ω_0 is the frequency in dimensionless form. The interval of existence of two

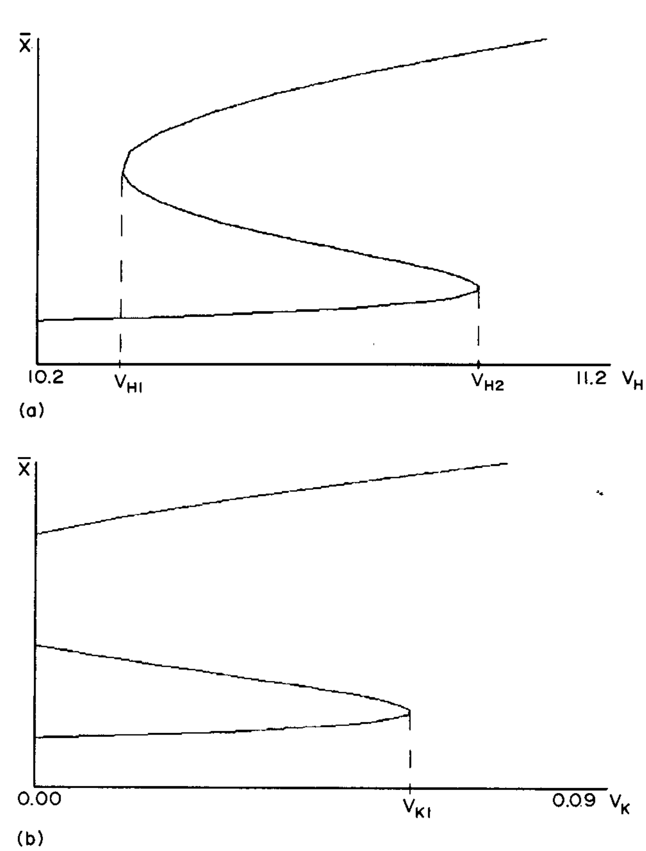

Fig. 4. Bifurcation diagram. (a) Dependence of steady-state dimensionless proton concentration $\bar{x}$ on the V_H (proton influx rate into near-membrane region). In the area between $V_{H1} = 10.34$ and $V_{H2} = 10.94$ there are three steady states. In the area $V_H < V_{H1}$ there is one steady state (1) and in the area $V_H > V_{H2}$ there is one steady state (3). Parameters used: $V_k = 0.0325$, $a = 26.44$, $b = 0.696$, $k_H = 1$. (b) Dependence of steady-state dimensionless proton concentration $\bar{x}$ on the V_K (potassium ion influx rate into near-membrane region). In the area $V_{K1} < 0.065$ there are three steady states. In the area $V_K > V_{K1}$ there is only one steady state (3). Parameters used: $V_H = 10.637$, $a = 26.44$, $b = 0.696$, $k_H = 1$.

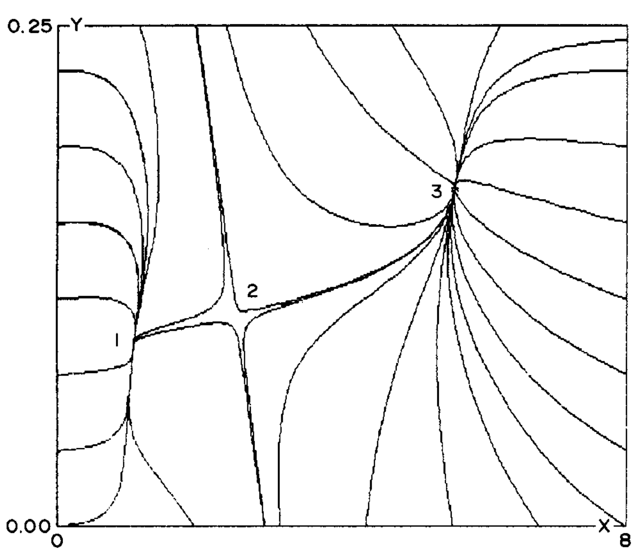

Fig. 3. Phase diagram of a bistable system [8]. x, y = Dimensionless variables for proton and potassium ion concentrations, respectively. States (1) and (3) are stable, state (2) is unstable. With $V_H = 10.637$, $V_K = 0.0325$, $a = 26.44$, $b = 0.696$, $k_H = 1$, the system has two stable states, $\bar{x}_1 = 1.08$, $\bar{y}_1 = 0.09$, $\bar{x}_3 = 5.59$, $\bar{y}_3 = 0.17$.

critical values of frequency, discussed above, in dimensional form is $f = 6.2–12.7$ Hz. The applied field intensity is about 600 V cm^{-1}.

Thus, the multi-stationary membrane system can be regulated by a periodic electric field of small amplitude. There are critical frequencies at which the system is switched from one steady state to the other.

2.3. *Effect of a weak electric perturbation on a self-sustained oscillatory system*

Under some conditions, the non-linear ion transfer system may go into self-sustained oscillations. A configuration of ion flux leading to self-sustained oscillation is the following. Let us assume that ions are transferred only as THK^+ complexes. Complexes TH,

$(TH^2)^+$ and TK are inactive and are not transferred across the membrane.

The antiport diagram appears as shown in Eq. (11).

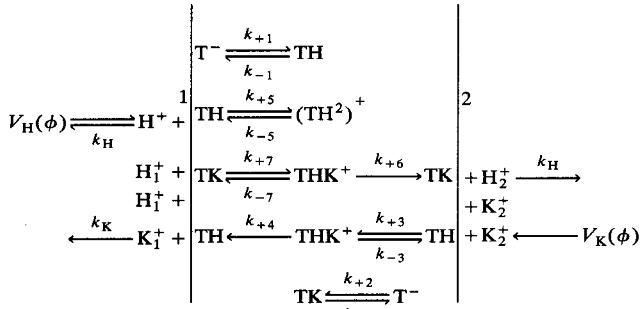

(11)

where subscripts 1 and 2 on the ion concentrations represent the sides of the membrane and $k_{\pm i}$ ($i = 1, 2, \ldots, 7$) are rate constants of the ion transfer stages. Using a system of equations analogous to Eq. (2) and making simplifications, one obtains a system of two differential equations for dimensionless variables:

$$\mathrm{d}x/\mathrm{d}\tau = V_H - k_H x - zbxy/[1 + b(x + xy + y) + cx^2]$$

$$\mathrm{d}y/\mathrm{d}\tau = V_K - bxy/[1 + b(x + xy + y) + cx^2] \qquad (12)$$

where $a = \bar{K}_m k_{+6}/(K_m k_{+4})$, $\bar{K}_m = (k_{-3} + k_{+4})/k_{+3}$, $K_m = (k_{-7} + k_{+6})/k_{+7}$, $b = \bar{K}_m k_{+2}/k_{-2}$, $c = K_m^2$ $k_{+1}k_{+5}/k_{-1}k_{-5}$.
Within the definite range of the parameters of the system, the solution may be a limit cycle.

The coordinates of the unstable equilibrium point are

$$\bar{x} = (V_H - V_K a)/k_H$$

$$\bar{y} = V_K(1 + b\bar{x} + c\bar{x}^2)/[b(\bar{x} - V_K - V_K\bar{x})]$$

With an applied perturbation, the system of Eq. (12) takes the form

$$\mathrm{d}x/\mathrm{d}\tau = V_H(1 + A \sin \omega t) - k_H x$$
$$- abxy/[1 + b(x + xy + y) + cx^2]$$

$$\mathrm{d}y/\mathrm{d}\tau = V_K(1 + A \sin \omega t)$$
$$- bxy/[1 + b(x + xy + y) + cx] \qquad (13)$$

To investigate the functional properties of a self-sustained oscillatory system, we made a bifurcation analysis and investigated the influence of the applied electric field on the system parameters. Varying the proton inflow rate V_H with the rest of the parameters fixed yields the bifurcation picture shown in Fig. 6. With $V_H = 0.5241$ in the system of Eq. (12) damped oscillations are generated. The steady-state point here is the stable focus (Fig. 6(b), curve A). With $V_H = 0.5243$, Hopf's bifurcation takes place, and a limit cycle is

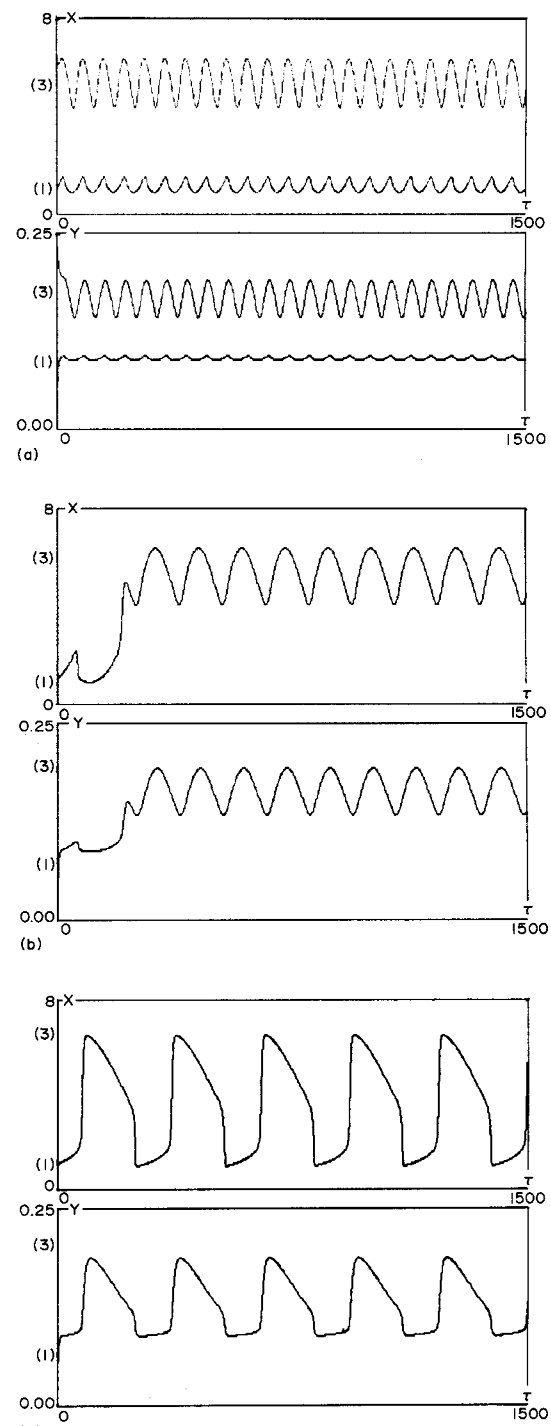

Fig. 5. Computer simulation of kinetics of a bistable K^+/H^+ antiport system. x, y, τ = Dimensionless variables of the system for proton $[H^+]$ and potassium $[K^+]$ concentrations and time, respectively. (a) With fixed amplitude of external field ($A = 0.03$) and relatively high frequency ($\omega = 0.1$), small-amplitude concentration oscillations take place in the neighbourhood of state (1) or (3). (b) With lower frequency of applied field, $\omega_1 = 0.047$ (the first critical magnitude), the system possesses only one steady state (3). If the movement starts near the point (1), parametric triggering to state (3) takes place. (c) With the frequency of applied field $\omega_2 = 0.023$ (the second critical point), concentration oscillations between two steady states (1) and (3) occur. Parameters used: $V_H = 10.637$, $V_K = 0.0325$, $k_H = 1$, $a = 10.44$, $b = 0.696$.

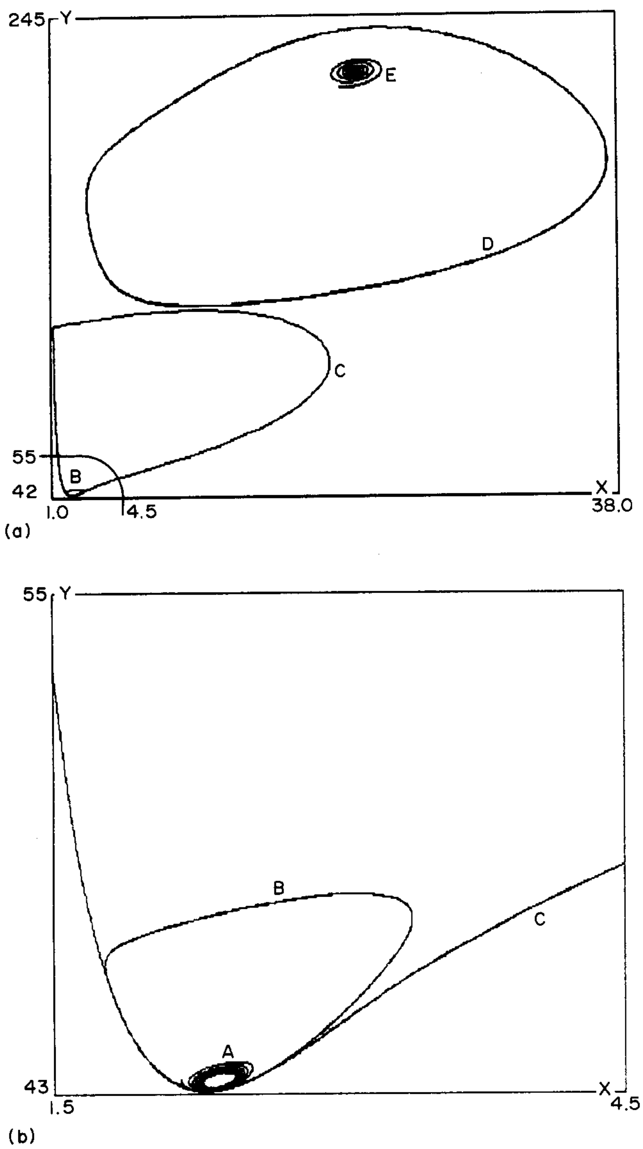

Fig. 6. Phase diagrams of the system of Eq. (12) with variation of the control parameter V_H (proton influx rate into near-membrane region). (a) Overall scheme. (b) Enlargement of the bottom-left region of (a). With $V_H = 0.5241$ the steady state is the stable focus ((b), curve A). With $V_H = 0.5243$, a limit cycle is generated ((a, b), curve B). The cyclic amplitude is small at first: $\Delta x = 0.65$, $\Delta y = 1.4$ (x, y are dimensionless proton and ion concentrations, respectively) but increases with increase in V_H. For $V_H = 0.5245$, the amplitude of natural oscillations increases drastically: $\Delta x = 18$, $\Delta y = 78$ ((a, b), curve C) and then increases slightly until $V_H = 0.7$ ((a), curve D). With $V_H = 0.71$, a stable focal point appears in the system again ((a), curve E). Parameters used: $V_K = 0.5$, $k_H = 0.01$, $a = 1$, $b = 1$, $c = 10$.

generated (Fig. 6(a,b), curve B). The cyclic amplitude is small at first, $\Delta x = 0.65$, $\Delta y = 1.4$ (x, y are dimensionless proton and potassium ion concentrations, respectively), but increases with V_H. For $V_H = 0.5244$, $\Delta x = 1$, $\Delta y = 2.5$ For $V_H = 0.5245$, the amplitude of natural oscillations increases drastically: $\Delta x = 18$, $\Delta y = 78$ (Fig. 6(a,b), curve C) and then increases slightly until $V_H = 0.7$ (Fig. 6(a), curve D). With $V_H = 0.71$, a stable focal point appears in the system again (Fig. 6(a), curve E).

A can be seen, the region in which bifurcations appear is very narrow: a change in parameter by 10 000 fractions produces new behaviour patterns, from damped oscillations to limit cycles of different amplitudes. The effect of an external periodic electric field was considered close to the bifurcation lines and within the ranges of the parameters far from the bifurcation. With $V_H = 0.5241$, which corresponds to the stable focal point, and the amplitude $A = 0.0005$ (corresponding to a field intensity of 10 V cm^{-1}) and cyclic frequency $\omega = 0.005$ (corresponding to a field frequency of 1.4 Hz) of the applied field, the system goes into resonance, similar to what was described above for a resonant system (Eq. (6)). Increasing the amplitude to $A = 0.001$ (corresponding to 20 V cm^{-1}) leads to different effects. With $\omega < 0.005$, a limit cycle with a small amplitude is generated. On increasing the frequency above this value, a limit cycle with large amplitude is generated. With $\omega = 0.02$ (5.6 Hz), the cycle disappears. Thus, at some amplitude of applied electric field, varying the frequency causes oscillations of various amplitudes or stops them.

In an applied electric field, the rates of influxes beyond the bifurcation point are kept stable. With $V_H = 0.65$ and amplitude $A < 0.1$ of the applied field, no significant changes in the amplitude of concentration oscillations are observed. Only a phase shift takes place. With $A = 0.1$ (corresponding to 2000 V cm^{-1}) one observes a resonance-induced increase in the concentration oscillation, by a factor of 1.2 for x (proton concentration) and 1.7 for y (potassium ion concentration). With frequencies higher than resonance frequencies, the applied periodic field modulates the oscillations, its amplitude changing little.

We also investigated the influence of the initial conditions and phase of the applied perturbation. The amplitude of the concentration oscillations remained unchanged. Hence, beyond the bifurcation point, the applied electric field causes a phase shift in the natural oscillations and is almost without effect on the amplitude.

It appears that beyond the bifurcation point a self-sustained oscillatory system of transmembrane ion transport with certain values of parameters is very stable to weak electric perturbations. Noticeable changes appear when the amplitude of the applied field is at least 2000 V cm^{-1}. With the values of the parameters being close to the bifurcation points, the applied electric field of small amplitude of 20 V cm^{-1} causes significant effects.

3. Discussion

We have investigated three mathematical models of ion exchange in the membrane, described by nonlinear differential equations. The solutions for different parameters are in good agreement with the phenomena observed in weak applied electric fields in living systems. From the experimental results and comparison of the responses of live systems to the electric perturbation with model results, we can gain insight into the underlying mechanisms without resort to special field-sensitive structures, because the inherent nonlinearity of biological systems can result in a variety of responses.

As an illustration, the release of Ca^{2+} from cerebral tissue under the effect of electromagnetic fields [22], or the intensification of ion flows driven by K/Na ATPase [15–17] at optimum frequencies, beyond which the effect is less expressed, correspond to the resonance mechanism of the response described with the first model. The term "resonant response" is widely used by investigators with respect to electronic, nuclear and other types of resonance. In our case, we speak of a resonance at the organization level of the system. A biological system can be arranged as a kind of a nonlinear amplifier, such as is used in radioelectronics. A comparison with this device may help to make clear not only the resonant effect of an applied field but also the informational character of its interaction with a biological system. By analogy, a radio signal containing some piece of information has a very low energy compared with the energy of the power supply unit in a radioelectronic device.

Another type of response, switching in a bistable system, characterizes the effects of applied variable electric field used in clinical medicine. Processes that may arise in such situations are described by the second model. In the case of a therapeutic effect, one considers an organism to have two stable states, a healthy and a pathological one, with different times of direct and backward transitions. If such occurs, there is an optimum frequency range for a field within which it can switch an organism from the pathological to the healthy state. Within this frequency range, no reverse switching occurs. This also explains why an organism, being initially healthy, does not switch to the pathological state in an applied electromagnetic field having such frequencies. As follows from our model, one may expect that there are lower frequencies at which an organism may alternatively be in either a healthy or a pathological state. Perhaps this may account for the effects of the extremely low frequency of technological and natural environmental electromagnetic exposures on humans.

The last type of nonlinear response treated here is the response of a self-sustained oscillatory system. Many authors believe that the rhythms of biological systems of endogenous origin or rhythms imposed by external exposures are very important for the normal development of many vital processes [25]. The cessation of rhythmic activity or phase shift in the rhythms may deteriorate the biological functions. The regulation of the rhythmic activity by applied electric fields can produce curative effects. To correct the phase of the rhythms (for instance, impaired cardiac rhythms [26]), the amplitude of the applied field has to be fairly large. This corresponds to a situation where the field acts far away from the bifurcation boundary. To initiate oscillations in the vicinity of the bifurcation boundary, the amplitude may be lower by a few orders of magnitude.

The mathematical models discussed here allow one to explain the effects of low-frequency and low-amplitude fields observed in experiments and used in therapeutic practice.

To conclude, we should note that an important problem is the capability of a biological system to distinguish the periodic signals against the natural electromagnetic background noise. The preliminary data obtained by us show that owing to the nonlinear arrangement, the system can function as a nonlinear filter detecting useful signal-containing information. This aspect will be considered in a following paper.

References

[1] M. Blank, Bioelectrochem. Bioenerg., 13 (1984) 93.
[2] M. Blank, Biochim. Biophys. Acta, 906 (1987) 227.
[3] M. Blank, J. Electrochem. Soc., 134 (1987) 1112.
[4] M. Blank and R. Goodman, Bioelectrochem. Bioenerg., 19 (1988) 569.
[5] T.Y. Tsong, D.-S. Liu, F. Chauvin, A. Gaigalas and R.D. Astumian, Bioelectrochem. Bioenerg., 21 (1989) 319.
[6] V.S. Markin and T.Y. Tsong, Bioelectrochem. Bioenerg., 26 (1991) 251.
[7] A.S. Presmann, Electromagnetic Fields and Living Nature, Nauka, Moscow, 1968, p. 9 (in Russian).
[8] F.A. Popp, U. Warnke, H.L. König and W. Peschka (eds.), Electromagnetic Bio-Information, Urban und Schwarzenberg, Munich, 1989.
[9] G.Yu. Riznichenko, T.Yu. Plusnina, T.N. Vorob'eva, S.I. Aksyonov and G.M. Tcherniakov, Biofizika, 38 (1993) 667.
[10] T.Yu. Plusnina, G.Yu. Riznichenko, S.I. Aksyonov and G.M. Tcherniakov, in press.
[11] V.S. Markin, T.Y. Tsong, R.D. Astumian and B. Robertson, J. Chem. Phys., 93 (1990) 5062.
[12] R.D. Astumian and B. Robertson, J. Chem. Phys., 91 (1989) 4891.
[13] W.R. Adey and A.F. Lawrence (eds.), Nonlinear Electrodynamics in Biological Systems, Plenum Press, New York, 1984.
[14] R. Cadossi, G.B. Ceccherelli, G. Emlia, G. Torelli, M.P. Ruggieri, F. Bersani, A. Cossarizza and Franceschi, Bioelectrochem. Bioenerg., 19 (1988) 315.
[15] E.H. Serpesu and T.Y. Tsong, J. Membr. Biol., 74 (1983) 191.
[16] E.H. Serpesu and T.Y. Tsong, J. Biol. Chem., 259 (1984) 7155.
[17] D.-S. Liu, R.D. Astumian and T.Y. Tsong, J. Biol. Chem., 265 (1990) 726.
[18] M. Toro and E. Arst, J. Membr. Biol. 95 (1987) 1.
[19] V.S. Markin, V.S. Sokolov, L.I. Boguslavsky and L.S. Yaguzhinsky, J. Membr. Biol., 25 (1975) 23.
[20] Yu.N. Antonenko and L.S. Yaguzhinsky, Biol. Membr., 5 (1988) 718.

[21] K.J. McLeod, R.C. Lee and H.P. Ehrlich, Science, 236 (1987) 1465.
[22] S.M. Bawin and W.R. Adey, Proc. Natl. Acad. Sci. USA, 73 (1976) 1999.
[23] M. Blank and L. Soo, Bioelectrochem. Bioenerg., 24 (1990) 51.
[24] M. Blank and L. Soo, Bioelectrochem. Bioenerg., 28 (1992) 291.
[25] R.M. Zaslavskaya, Chronodiagnostics and Chronotherapy, Medictsina, Moscow, 1991 (in Russian).
[26] L. Glass and M.C. Mackey, From Clock to Chaos, Mir, Moscow, 1991, p. 134 (in Russian).